

Detection of Soil Water Content Using Continuous Wave Ground Penetrating Radar

Sonal Oimbe [#], Rahul Ingle ^{*}, Raval Awale ^{*}

[#] TE connectivity Ltd, Pune, India.

^{*} Electrical Engineering Department, VJTI Mumbai-400019, India.

E-mail: aboimbe@gmail.com, rringale@vjti.org.in, rnawale@vjti.org.in

Abstract— In this work, continuous wave ground-penetrating radar (CW-GPR) has been used for detecting the soil water content in context to farm management. It is here speculated that CW-GPR utilized to observe variations in Soil parameters in different geographical area where traditional methods fails such as reflection-based GPR method. An experiment was performed on different farms in and around Mumbai city locality in a 20 * 14 m section of natural grassland at the SAMEER- IIT BOMBAY Research Facility in Mumbai city, INDIA. Two survey methods such as velocity analysis and GPR reflection surveys of ground wave were inefficient at the experiment site due to the signal attenuation which is related with the clay-rich soil. CW-GPR data sets were collected on regular and daily basis during a 5-d period in February 2017. The samples of soil were collected for analysis purpose from the mentioned geographical area. The clear response has been observed for early time signal amplitude to changes in soil water content using CW-GPR data. The strong correlation has been observed between the GPR data sets with Soil water content, which is uniform with the CW-GPR dependence on relative permittivity. The outcome reveals that the CW-GPR method can be utilized to acquire spatially distributed information on subsurface moisture content in clay-rich soils.

Keywords— Continuous Wave Ground Penetrating Radar (CW-GPR), Time Domain Reflectometry (TDR), Soil Water Content (SWC), average envelope amplitude (AEA).

I. INTRODUCTION

A. Basics of spatial distribution

Finding water content in Soil is critical and tedious task using biological and chemical processes. Various literatures pointed the importance soil water content (SWC) measurement in detail [26, 20]. However, conventional techniques have remarkable limitations of estimations of soil water content. Several techniques such as time-domain reflectometry (TDR) and soil sampling which are noninvasive in nature can impede with the processes being studied. Both the technique cannot easily give dense estimates and point measurement for SWC and also these are bit expansive techniques. However, SWC collected by satellite and cosmic ray probe doesn't easily allow field-scale process analysis [7, 15].

The best feasible solution for all the above mentioned problems is Continuous Wave Ground-penetrating radar (CW-GPR). This technique has been used as a tool for SWC measurement at the experimental field with the help of reflection data, borehole transillumination data, ground wave

data [2,8,10,12,13,17,21,25]. These methods are noninvasive in nature and can efficiently used for data collection on large field areas for SWC estimation in vadose zone. Moreover, ground wave and Reflection analysis have several limitations. Conventional reflection analysis demand reflector observation at a familiar deepness for calculating the two-way travel time [9]. Similarly, in ground wave analysis, operator required to detect the antenna offset such that ground wave does not interfered with the airwave reflection in spite of changes in SWC and field site. Both of these techniques are impeded by large clay content and large conductive soils which resulted in signal attenuation

The proposed CW-GPR method uses Ground Penetrating RADAR which is an alternative approach to estimate variations of SWC at the field scale [18,19]. In this method, variation of ground as well air wave are used together to detect the variation in Electromagnetic properties near surface. The statistical parameter called as Average Envelope Amplitude (AEA) permits us to observe and analyze the variation in amplitude systematically. Most of the times it is called as "average envelope" or "envelope amplitude" [5,6,18]. Whenever there is combination of air and ground waves, this method can be used. As this method,

doesn't depend on reflection phenomenon hence near-surface reflector is not required. This CW-GPR method can be efficiently used for clay-rich field site also. The other available method fails due to excessive signal attenuation.

In this method, CW-GPR used to observe variation in SWC using time-lapse measurements pre and post irrigations at clay-rich field site. This method can also be applied at the experimental field where attenuation is higher.

B. An Overview of GPR

In CW-GPR two antennas are used. One for transmission and other for reception purpose. In transmission antenna, short pulsed electromagnetic signal is transmitted and the receiving antenna receives transmitted signals and measure transmitted and reflected energy from the field area. The signal transmission takes place through air and different subsurface with different velocities, different materials with different permittivity. The ratio of the absolute permittivity of the substance to permittivity of free space or vacuum is the relative dielectric permittivity (ϵ_r) of the air and the substance. As the water content in the soil has remarkable effect on ϵ_r , hence the most effective tool to study moisture in the soil is CW-GPR. The relative permittivity of fresh water, air and mineral soil grains is 80, 1, and 4 respectively. In fact very small variation in water content can bring considerable variation in ϵ_r [24]. In addition, water has different conductivities depending on the different minerals present in water which is responsible for signal attenuation [4].

The ϵ_r is related to the wave velocity by,

$$v = \frac{c_0}{\sqrt{(\mu_r \epsilon_r / 2)[(1 + p^2) + 1]}} \quad (1)$$

Where v represent wave velocity, c_0 : speed of light in free space, μ_r : relative magnetic permeability of the material, $\mu = \mu_r \mu_0$ where μ_0 is the magnetic permeability in a free space, μ_r is 1 for most common Earth soils, and p is a loss factor given by:

$$p = \frac{\sigma}{\omega \epsilon} \quad (2)$$

Here σ : conductivity of the material, ω : the angular frequency, ϵ : represented by $\epsilon = \epsilon_0 \epsilon_r$, where ϵ_0 is the permittivity of a free space.

Reflection and Ground wave based methods use Eq. [1] for relative permittivity ϵ_r estimation by counting GPR signal travel time from the transmitter to the receiver through the shallow subsurface and the signal that reflects off subsurface interfaces where there is a ϵ_r contrast [12]. Using pedotransfer function, the permittivity value can be converted into SWC estimate [23].

The Conventional methods using GPR are restricted in large-conductivity material, such as saline pore fluids based materials and clay-rich soils. The relation of attenuation coefficient of GPR (α) to ϵ and σ is given by,

$$\alpha = \omega \sqrt{\frac{\mu \epsilon}{2} \left(\sqrt{1 + \frac{\sigma^2}{\epsilon^2 \omega^2}} - 1 \right)} \quad (3)$$

Small amplitude GPR signal is more often attenuated in highly conductive soils even before it reaches the receiver.

C. CW- GPR Early-Time Method

The recently proposed methodology for CW-GPR is the analysis of Early-time amplitude [19]. This yield an alternative method to extract information on variations in SWC from common-offset GPR surveys. The advantage of this method is that the GPR antenna offset doesn't need to be big. This indicates that, this method works very well with commercial bistatic common-offset antenna equipment with inseparable antennae. This method collect amplitude information easily as it is responsive to conductivity or/and permittivity or/and changes at shallow depth. During the analysis in a GPR reflection survey, the beginning part of the signal is the blend of air and ground waves and they are analyzed without separated in time [5]. By analyzing both field and modelled data of early-time signal, variations in CW-GPR's amplitude attributes were able to map near-surface changes in ϵ_r [5]. Hence this method is highly capable of mapping SWC when field calibration can be executed using distinct point measurements.

Nowadays this method has been widely used to decide its efficacy [18]. In this method, a tank is built using polyvinyl chloride material. Its bottom is filled with a layer of gravel which is then followed by layer of river sand above. Pipes are kept in the gravel layer to pour incremental water inside the tank. This will allow observing the variation in early time CW-GPR signal as the water proceeds towards the surface. In this way it is concluded that,

- (i) The outcome of the measurement of GPR Signal was in line with preceding numerical model by [5, 19].
- (ii) The AEA and Dielectric constant of SWC are correlated inversely with each other.
- (iii) The wavelength of the GPR signal and the subsurface thickness affecting the early time signal is on the same order.

The amplitudes of the air wave ($A_{air-wave}$) and ground wave ($A_{ground-wave}$) are given as [5].

$$A_{air-wave} = \frac{\sqrt{\epsilon_0 \mu_0}}{2\pi \epsilon_0 (\epsilon_r - 1) S^2} \quad (4)$$

$$A_{ground-wave} = -A_{ground-wave}^0 \exp \left[\left(-\frac{1}{2} \right) \frac{\sqrt{\mu_0}}{\epsilon_0 \epsilon_r} \sigma S \right] \quad (5)$$

Where

$$A_{ground-wave}^0 = \frac{\sqrt{\epsilon_r \mu_0}}{2\pi\epsilon_0(\epsilon_r - 1)S^2} \quad (6)$$

Where μ_0 : Magnetic permeability of vacuum, ϵ_0 : dielectric permittivity of vacuum, σ : soil electrical conductivity, A^0 : amplitude of the ground wave in a vacuum, S : antenna separation.

Eq. [5] represent the exponential term. This term is evanescent portion of the ground wave that propagates, decaying, above the surface [1]. Early-time CW-GPR method has a limitation that it is a tedious task to find out the effect of variations of conductivity and permittivity on early-time GPR signal amplitude. Even though the effect of each property has been analysed separately in controlling setting on early-time GPR signal [3]. From equation [4-6] it is clear that, the relative direct GPR signal amplitude is affected by both conductivity and permittivity of subsurface.

Some of the literatures suggested that permittivity affects early-time amplitude [5]. Moreover, negative impact on envelope amplitude is seen by high-conductivity materials using statistical parameters for relating GPR signal to relative permittivity. The potentially tougher alternative is proposed as an alternate statistic, which is “carrier frequency amplitude”.

II. METHODS

A. Description of field site

Society for Applied Microwave Electronics Engineering & Research (SAMEER) is located in IIT Bombay campus, India (Fig. 1). This property is used for Research projects of various environmental, ecological, educational and engineering programs. In support of this aim, a wide area of this property is reserved as a typical forest area. This site is located near Powai Lake, hence this site has clay rich soil. Some region contains clay contents up to 60%. This clearly indicates that conventional GPR methods are not effective to characterize at this site. The motivation for testing the early-time method at this site was a combination of spatial soil moisture and clay-rich soil data. This study focused on an area in the East-west corner of SAMEER, IIT Bombay, where there is a relatively flat area for experiment. We selected a 20*14 m portion of this area for geophysical and irrigation measurements.



Fig.1 Experimentation Area of the SAMEER, IIT Bombay Research Facility Mumbai, India.

B. Characterization of the Background

After site selection, various geophysical measurements have been performed to get better knowledge about the subsurface. Initially CW-GPR wide-angle refraction and reflection survey have been collected (Fig.2). Then common-offset measurement of GPR has been selected for selected path to identify the optimal GPR settings for the site (Fig.3).

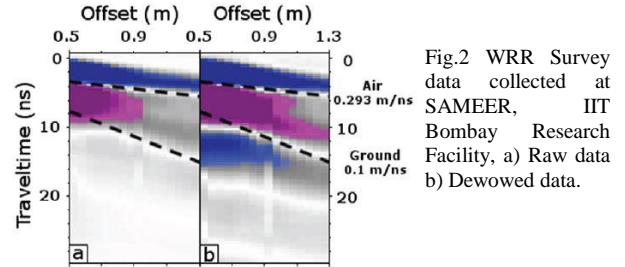


Fig.2 WRR Survey data collected at SAMEER, IIT Bombay Research Facility, a) Raw data b) Dewowed data.

The GPR signal data has been collected from antenna of 200MHz range and 1-m separation. It has a pulsar voltage of 400 V. The GPR moved along the transect to accurately position measurements every 5 cm hence the odometer wheel which was attached to the Smart Cart. For both WARR and common-offset measurements 0.2-ns sampling interval was used.

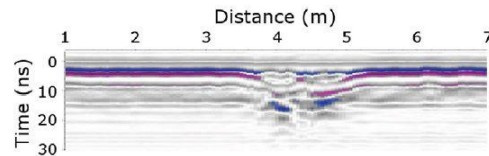


Fig.3 Data collected on 12 Feb 2017 from Common-offset 200-MHz GPR line with 5-cm step size at the SAMEER, IIT Bombay Research Facility.

WARR survey has been already collected on the site (11 Jan) before the commencement of main experiment as shown in Fig.2. Air wave is clearly appeared in the raw and gained data while ground wave appeared only after gain data. Then dewow were applied and the linear gain has been increased manually from 2.5 dB to 15 dB during the duration from 0 to 30ns. But attenuation still continued to the point which was difficult to pick up by maximum offset. There was no visibility of reflections in the data down to 30 ns.

Common offset survey result collected on 12 Feb shown in Fig. 3. The combination of air and direct ground waves is the overlapping waves at the beginning and end of the line for the direct signal. 120 L water is used to wet the 1*1 m field segment in the centre of the line. This results in the distraction to ground wave due to which it slows down and got separated from the air wave. This separation is not uniform across the wide range of SWC values. It is difficult to find out the first break. However, this separation cannot be maintained across a wide range of Soil Water Content values, and the first break is difficult to identify. Still there was no visibility of reflections in the data down to 30 ns.

C. Data Collection and the Instrumentation in the field

The scheduled of the measurement and irrigation is shown in Table 1. On Day 1 the experimental field area was irrigated at night using simple garden sprinkler. The setting of the sprinkler arranged in such as way that sprinkler spraying water into the area along the edge and in a 180° arc, to a distance of approximately 8 m. The rate at which water was sprinkle from sprinkler was the 2.5 cm/hour at a radius of 3 m from the sprinkler. The total duration for sprinkler was 6 hour starting at 2.00 PM. Additionally, three 1*1 m fully filled water tank of 100 L capacity were kept near field area at 2:00 PM on Day 1. The complete infiltration of the water was allowed before the water tanks were removed from the area. This result in high water content in small area surrounded by dry soil.

TABLE 1:

CHART INDICATING DAY 1 TO DAY 5 SCHEDULE OF TDR AND GPR SURVEY FROM SITE.

| Event | Day 1 | | Overnight | Day 2 | |
|---------------|-------|----|-----------|-------|----|
| | AM | PM | | AM | PM |
| TDR | | × | | × | |
| GPR | × | | | × | |
| Irrigation | | | × | | |
| Soil Sampling | | | | | |

| Event | Day 3 | | Day 4 | | Day 5 | |
|---------------|-------|----|-------|----|-------|----|
| | AM | PM | AM | PM | AM | PM |
| TDR | × | | × | | × | |
| GPR | × | | × | | × | |
| Irrigation | | | | | | |
| Soil Sampling | | | | | | × |

In this work continuous GPR signals is measured at 9AM daily from Day to Day 5. As shown in Fig.4, Each data set consisting of 15 lines of 1m spacing and a length of 20 m. Data is collected for nearly 1 hour. Here GPR is set up to collect these data for the 2 July common-offset measurement except with a 0.5-m antenna separation instead of 1m so that ground and air wave overlap takes place during entire duration of experiments and all level of saturation.

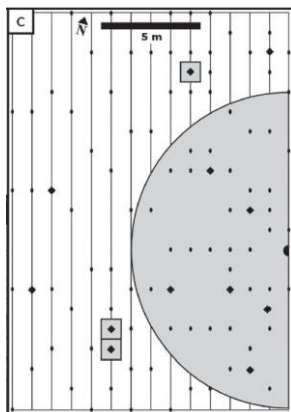


Fig.4 14*20 m area for experimental setup.

In Fig. 4, FPR transect indicated by Vertical lines, TDR locations are indicated by ovals, and diamonds indicates the locations of pair of soil sampling (where TDR measurements were also collected). Sprinkler area is represented by the large gray semicircle, and the water tank represented by gray squares.

The TDR data collected in synchronization with CW-GPR data sets, during morning timing around 10 AM with the help of soil water measurement system (Hydro Sense CS620) using a two-rod probe having rod size of 12cm. This system finds out the mean duration output from the probe τ , in milliseconds. They varied due to ϵ_r of the subsurface which depends on the SWC. Nearly 100 TDR points have been collected each day which was focused for the geographical area chosen for soil samples collections. These areas chosen to give the maximum possible scope of wetting state: Complete dry soil, soil within the water tank location, and around the 3m to 6 m from the sprinkler area. The data collection for TDR approximately taken 90 minutes.

Soil samples were collected on the day 5 of measurements; from 24 Geographical areas at the depth of 5* 10 cm and 15*20 cm. These depths were selected just to avoid the maximum root zone of grassland soil and to reduce the evapotranspiration effects during the complete course of the day. The samples of the soil were collected with the help of soil sampling ring. This soil samples then bagged in plastic bag. Then these soil samples stored in refrigerator of laboratory within 2 hours after collecting it. Gravimetric Water Content is calculated for 48 soil cores after drying soil samples in oven [16].

D. Data Processing

Each line has 400 measurements for CW-GPR surveys. A moving average was applied before processing data in blocks of seven. After averaging each data, it will denotes the part of the transect around 0.35m in length and crossing 30 cms of data points before and after it. These collected data then normalized and averaged for avoiding the small variations from each and every data blocks. This results in ground coupling of GPR antennae in thick grassland.

The mathematical function called Hilbert transform were applied on all averaged measurements during first positive half cycle as positive as shown in Fig.5. MATLAB is used for data processing and it has built-in function for Hilbert Transform [5]. Each averaged CW-GPR data passed through this Hilbert Transform. The Hilbert transform is given by

$$\hat{x}(t) = \frac{1}{\pi} \int_{-\infty}^{\infty} \frac{x(s)}{t-s} ds \quad (7)$$

Here, $\hat{x}(t)$: Hilbert transform of the function $x(s)$, and the integration is the Cauchy principle value integral. The Hilbert transform gives the imaginary part of the complex GPR trace. The acquired CW-GPR signals indicated the real part of the trace. The calculations of the trace envelope which is also known as the instantaneous amplitude is derived using the Hilbert Transform. by taking the absolute value of the transformed GPR signal [22].

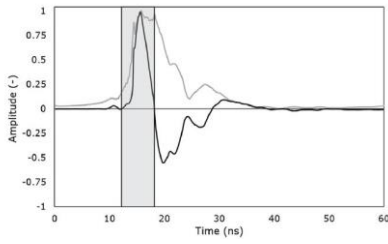


Fig .5 GPR traces Representation (using black colour) and its envelope (using gray colour) from a line collected in the experimental area. First positive half cycle is shown by grey colour Shaded area.

The first positive half cycle is used to provide greatest SNR of any portion of early time continuous GPR signal which was extracted from a custom function [5]. The AEA is calculated using Hilbert transform of absolute value of measurements and integral of the result which is divided by unit length of the integral. This AEA is then inverted to be consistent with the work of [5,18]. For estimating an absolute value of GWC, there is an alternate methodology.

Here, experimental field site specific empirical relationship is established between TDR measurement τ and GWC values depend upon the soil cores of size 5cm to 10cm. This equation is used to convert all TDR measurements (of τ) into GWC values (in %). Nearly 11 to 22% of GWC is the values of TDR calibration, which surrounds most of the saturation levels noticed during the experimental study.

III. RESULTS

A. Time-Domain Reflectometry (TDR) results

The TDR data results collection is as shown in Fig. 6. After the Day 1, collected TDR data shows that average and median GWC are 13% in the field area where experiments are performed. Due to environmental a few areas have 15 % GWC. On the Day 2, there is an increased in the GWC after irrigation of experimental area. It is observed 13 to 20% GWC in the area which was 2 and 3 m from the sprinkler. Around 19 % GWC is observed at wet area. On Day 3, collected data is identical to Day 2 data set. There is a significant decrease in GWC values on Day 4 from 12% to 18 %. The area close to sprinkler has approximately 23 % GWC on Day 5.

B. Early-Time GPR Analysis and Soil Sampling

The results of the early time GPR analysis is shown in Fig.7. In this plot, AEA^{-1} of the first positive half cycle of the traces calculated by taking a mean of blocks of seven traces. On Day 1, averaged AEA^{-1} value of 5.91×10^{-5} . In fact it is observed that some area have few higher AEA^{-1} due to water leaking environmental effect around the edge. The initial data set collected after irrigation on Day 2. The values in the dry areas (unirrigated) were mostly stable from Day 1. In an irrigation area, the values of the AEA^{-1} varies from 6.6×10^{-5} to 1.26×10^{-4} .

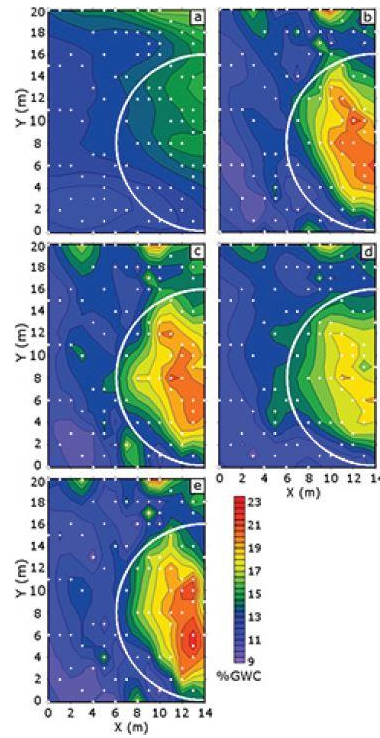


Fig.6 Day 1 TDR data sets is given in (a) using an interval of 0.5%, (b-e) shows Days 2 to 5 TDR data set, using a contour interval of 1% with the help of white diamonds which shows the location of measurement. Using linear variogram model the grid was acquired via kriging.

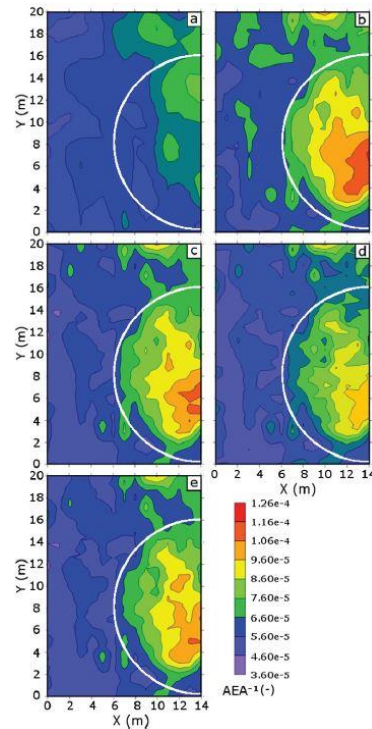


Fig.7 GPR inverted data (AEA^{-1}) data plotted in unit less amplitude units. (a) Day 1 (b) Day 2 (c) Day 3 (d) Day 4 (e) Day 5. The grid was acquired via kriging, using a linear variogram model.

Throughout the study duration, the values of the AEA^{-1} remained prominent. This is because of slow infiltration rate in clay rich soil. On the Day 2, the mean value of AEA^{-1} at experimental field was 7.10×10^{-5} , which reduced to 6.52×10^{-5} by the end of Day 5.

The Gravimetric analysis of soil cores result collected at the depth of 5 cm to 10 cms and 15cms to 20cms is shown in Fig. 8.

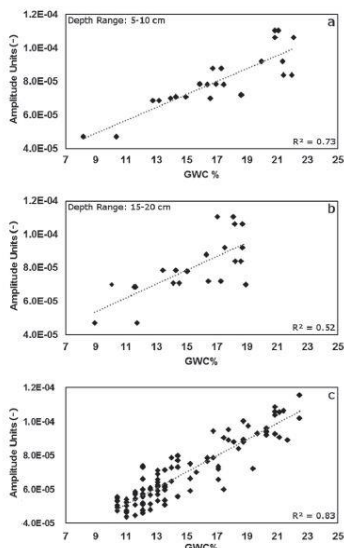


Fig.8 GPR inverted data AEA^{-1} plotted versus the GWC calculated from the samples of the soil collected via a sampling ring which is standard size at different depths such as (a) 5 cm to 10 cm and (b) 15cm to 20cm and (c) On Day 5, GPR inverted AEA^{-1} vs. TDR data points (101).

It is observed that at the depth of 15cm to 20 cm GWC samples ranged from 9 to 19%, and at the depth of 5cm to 10cm samples ranged from 8 to 22% GWC. Results during TDR τ , shows that the GPR signal travel time along the TDR rods, were changed to GWC by correlating the data at the depth of 2.45cm to 10cm soil core measurements acquired on Day 5 of the experiment. This relationship obtained is linear in nature:

$$GWC_{core} = 3.8297\tau + 0.2479 \quad (8)$$

IV. DISCUSSION

A. Discussion related with early time method and Background Measurements.

The ineffectiveness has been observed in SWC measurement in clay rich soil using the traditional GPR methods after initial measurement taken one before actual experiment. Even the WARR survey as shown in Fig. 2 reveals that ground and air wave methods are inefficient as it causes significant attenuation in clay rich soil. Even reflection method is not useful since no reflections are visible below the direct signal. Hence, the early-time CW-GPR technique is appeared as a viable GPR methodology which is mapping the spatial variability in shallow SWC at this experimental site.

The plot of GPR AEA^{-1} data and values of soil core GWC gives the most expected relationship as shown in Fig. 8a and Fig.8b, which proved that the early-time CW-GPR method is best technique to use GPR in clay rich soils which maps variations in GWC. In an areas where irrigation done on frequent basis, it is observed significant jump in AEA^{-1} in context with outputs of previous researchers [6,18]. It is also observed that AEA^{-1} values decreases at the end of the experiment which indicates small amount of infiltration and evapotranspiration occurs beneath the GPR influenced region.

In fact it is very much unfortunate to see that early time CW-GPR method is not viable to differentiate variations in conductivity from variations in dielectric permittivity in the setting of an experimental region. The irrigation water may

have various electrical conductivity prior to irrigation. Observing Electrical resistivity in context with CW-GPR could be useful to isolate variations due to dielectric permittivity. Indeed, the good correlations as shown in Fig.8 reveal that CW GPR AEA^{-1} values could be changed to values of GWC using a calibration equation.

There is an increase in GWC from Day 1 to Day 2 in the in the sprinkler-experimental area which is shown in TDR data. These data validate that the drift observed in the GPR data: also raising subsurface water content increased with AEA^{-1} as shown in Fig. 8c. Infact it is seen that CW-GPR and TDR data have better correlation than soil core data.

CONCLUSIONS

Early-time CW-GPR method is useful in the experimental area for finding the spatial variability in SWC from clay soils where other method fails to do this analysis. The traditional method such as WARR analysis and the analysis using common-offset ground wave were not able to provide a technique to measure the SWC at the experimental field site. CW-GPR AEA^{-1} increases with the corresponding increase with Irrigated areas of the experimental site. This is still unclear that whether the changes in the conductivity vs. permittivity results in the changes in the percentage change in AEA^{-1} ? Moreover, from the Gravimetric and TDR soil sample analysis it is very much clear that strong correlation exist between AEA^{-1} and independent GWC measurements. Best correlation is observed between the GPR data with the TDR data and soil core data at a distance of 5 to 10 cm. This result reveals that this method is sensitive to 15cm of the subsurface. Continuous soil cores from a wider area of the experimental region would improve our knowledge of the of investigation depth of CW-GPR. The CW-GPR early-time method opens up new opportunities of research using GPR in clay-rich soils and can benefit from further laboratory and field investigation.

ACKNOWLEDGMENT

We would like to thank VJTI and IIT Bombay for providing the facility to pursue the research in their Lab.

REFERENCES

- [1] Annan, A.P. 1973. Radio interferometry depth sounding: I. Theoretical discussion. *Geophysics* 38:557–580. doi:10.1190/1.1440360.
- [2] Cassiani, G., C. Strabbia, and L. Gallotti. 2004. Vertical radar profiles for the characterization of deep vadose zones. *Vadose Zone J.* 3:1093– 1105. doi:10.2113/3.4.1093.
- [3] Comite, D., A. Galli, S.E. Lauro, E. Mattei, and E. Pettinelli. 2016. Analysis of GPR early-time signal features for the evaluation of soil permittivity through numerical and experimental surveys. *IEEE J. Sel. Top. Appl. Earth Obs. Remote Sens.* 9(1):178–187. doi:10.1109/JSTARS.2015.2466174.

- [4] Davis, J.L., and A.P. Annan. 1989. Ground-penetrating radar for high resolution mapping of soil and rock stratigraphy. *Geophys. Prospect.*37:531–551. doi:10.1111/j.1365-2478.1989.tb02221.x.
- [5] Di Matteo, A., P. Elena, and S. Evert. 2013. Early-time GPR signal attributes to estimate soil dielectric permittivity: A theoretical study. *IEEE Trans. Geosci. Remote Sens.* 51:1643–1654. doi:10.1109/TGRS.2012.2206817.
- [6] Ferrara, C., P.M. Barone, C.M. Steelman, E. Pettinelli, and A.I. Endres. 2013. Monitoring shallow soil water content under natural field conditions using the early-time GPR signal technique. *Vadose Zone J.* 12(4). doi:10.2136/vzj2012.0202.
- [7] Franz, T.E., M. Zreda, R. Rosolem, and T.P.A. Ferre. 2013. A universal calibration function for determination of soil moisture with cosmic-ray neutrons. *Hydrol. Earth Syst. Sci.* 17:453–460. doi:10.5194/hess-17-453-2013.
- [8] Galagedara, L.W., G.W. Parkin, and J.D. Redman. 2003. An analysis of the ground-penetrating radar direct ground wave method for soil water content measurement. *Hydrol. Processes* 17:3615–3628. doi:10.1002/hyp.1351.
- [9] Gerhards, H., U. Wollschläger, Q. Yu, P. Schiwek, X. Pan, and K. Roth. 2008. Continuous and simultaneous measurement of reflector depth and average soil-water content with multichannel ground-penetrating radar. *Geophysics* 73:J15–J23. doi:10.1190/1.2943669.
- [10] Grote, K., S. Hubbard, and Y. Rubin. 2003. Field-scale estimation of volumetric water content using ground-penetrating radar ground wave techniques. *Water Resour. Res.* 39:1321. doi:10.1029/2003WR002045.
- [11] Hislop, G. 2015. Permittivity estimation using coupling of commercial ground penetrating radars. *IEEE Trans. Geosci. Remote Sens.* 53:4157–4164. doi:10.1109/TGRS.2015.2392110.
- [12] Huisman, J.A., S.S. Hubbard, J.D. Redman, and A.P. Annan. 2003. Measuring soil water content with ground penetrating radar. *Vadose Zone J.* 2:476–491. doi:10.2136/vzj2003.4760.
- [13] Huisman, J.A., C. Sperl, W. Bouten, J.M., Verstraten. 2001. Soil water content measurements at different scales: Accuracy of time domain reflectometry and ground-penetrating radar. *J. Hydrol.* 245:48–58. doi:10.1016/S0022-1694(01)00336-5
- [14] Karan, M., M. Liddell, S.M. Prober, S. Arndt, J. Beringer, M. Boer, et al. 2016. The Australia SuperSite Network: A continental, long-term terrestrial ecosystem observatory. *Sci. Total Environ.* 568:1263–1274. doi:10.1016/j.scitotenv.2016.05.170.
- [15] Kerr, Y.H., P. Waldteufel, J.P. Wigneron, S. Delwart, F. Cabot, J. Boutin, et al. 2010. The SMOS Mission: New tool for monitoring key elements of the global water cycle. *Proc. IEEE* 98:666–687. doi:10.1109/JPROC.2010.2043032.
- [16] Klute, A. 1965. Laboratory measurement of hydraulic conductivity of saturated soil. In: C.A. Black et al., editor, *Methods of soil analysis. Part 1. Physical and mineralogical properties, including statistics of measurement and sampling.* Agron. Monogr. 9. ASA, Madison, WI, p.210–221. doi:10.2134/agronmonogr9.1.c13.
- [17] Lunt, I.A., S.S. Hubbard, and Y. Rubin. 2005. Soil moisture content estimation using ground-penetrating radar reflection data. *J. Hydrol.*307:254–269. doi:10.1016/j.jhydrol.2004.10.014.
- [18] Pettinelli, E., A. Di Matteo, S.E. Beaubien, E. Mattei, S.E. Lauro, A. Galli, and G. Vannaroni. 2014. A controlled experiment to investigate the correlation between early-time signal attributes of ground-coupled radar and soil dielectric properties. *J. Appl. Geophys.* 101:68–76. doi:10.1016/j.jappgeo.2013.11.012.
- [19] Pettinelli, E., G. Vannaroni, B. Di Pasquo, E. Mattei, A. Di Matteo, A. De Santis, and A.P. Annan. 2007. Correlation between near-surface electromagnetic soil parameters and early-time GPR signals: An experimental study. *Geophysics* 72:A25–A28. doi:10.1190/1.2435171.
- [20] Robinson, D.A., C.S. Campbell, J.W. Hopmans, B.K. Hornbuckle, S.B. Jones, R. Knight, et al. 2008. Soil moisture measurement for ecological and hydrological watershed-scale observatories: A review. *Vadose Zone J.* 7:358–389. doi:10.2136/vzj2007.0143.
- [21] Rucker, D.F. 2011. Inverse upscaling of hydraulic parameters during constant flux infiltration using borehole radar. *Adv. Water Resour.* 34:215–226. doi:10.1016/j.advwatres.2010.11.001.
- [22] Taner, M.T., F. Koehler, and R.E. Sheriff. 1979. Complex seismic trace analysis. *Geophysics* 44:1041–1063. doi:10.1190/1.1440994.
- [23] Van Dam, R.L. 2014. Calibration functions for estimating soil moisture from GPR dielectric constant measurements. *Commun. Soil Sci. Plant Anal.*45:392–413. doi:10.1080/00103624.2013.854805.
- [24] Van Dam, R.L., and W. Schlager. 2000. Identifying causes of groundpenetrating radar reflections using time-domain reflectometry and sedimentological analyses. *Sedimentology* 47:435–449. doi:10.1046/j.1365-3091.2000.00304.x.
- [25] van Overmeeren, R.A., S.V. Sariowan, and J.C. Gehrels. 1997. Ground penetrating radar for determining volumetric soil water content: Results of comparative measurements at two test sites. *J. Hydrology* 197:316–338. doi:10.1016/S0022-1694(96)03244-1.
- [26] Vereecken, H., J.A. Huisman, H. Bogena, J. Vanderborght, J.A. Vrugt, and J.W. Hopmans. 2008. On the value of soil moisture measurements in vadose zone hydrology: A review. *Water Resour. Res.* 44:W00D06. doi:10.1029/2008WR006829.